

Articles

Identification of Novel Cyclooxygenase-2 Selective Inhibitors Using Pharmacophore Models

Albert Palomer,^{*,†} Francesc Cabré,^{†,§} Jaume Pascual,[†] Joaquín Campos,[‡] María A. Trujillo,[‡] Antonio Entrena,[‡] Miguel A. Gallo,[‡] Lluïsa García,[†] David Mauleón,[†] and Antonio Espinosa[‡]

R&D Department, Laboratorios Menarini S.A., Alfonso XII 587, 08918 Badalona, Spain, and Departamento de Química Orgánica, Facultad de Farmacia, Universidad de Granada, Campus de la Cartuja s/n, 18071 Granada, Spain

Received October 2, 2001

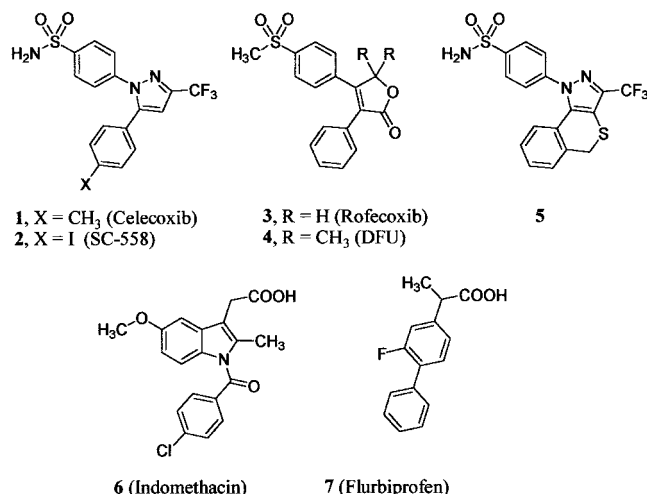
In the present study we have investigated whether pharmacophore models may account for the activity and selectivity of the known cyclooxygenase-2 (COX-2) selective inhibitors of the phenylsulfonfyl tricyclic series, i.e., Celecoxib (**1**) and Rofecoxib (**3**), and whether transferring this structural information onto the frame of a nonsteroidal antiinflammatory drug (NSAID), known to tightly bind the enzyme active site, may be useful for designing novel COX-2 selective inhibitors. With this aim we have developed a pharmacophore based on the geometric disposition of chemical features in the most favorable conformation of the COX-2 selective inhibitors SC-558 (**2**; analogue of Celecoxib (**1**) and Rofecoxib (**3**) and the more restrained compounds **4** (DFU) and **5**. The pharmacophore model contains a sulfonyl S atom, an aromatic ring (ring plane A) with a fixed position of the normal to the plane, and an additional aromatic ring (ring plane B), both rings forming a dihedral angle of $290^\circ \pm 10^\circ$. The final disposition of the pharmacophoric groups parallels the geometry of the ligand SC-558 (**2**) in the known crystal structure of the COX-2 complex. Moreover, the nonconserved residue 523 is known to be important for COX-2 selective inhibition; thus, the crystallographic information was used to position an excluded volume in the pharmacophore, accounting for the space limits imposed by this nonconserved residue. The geometry of the final five-feature pharmacophore was found to be consistent with the crystal structure of the nonselective NSAID indomethacin (**6**) in the COX-2 complex. This result was used to design indomethacin analogues **8** and **9** that exhibited consistent structure–activity relationships leading to the potent and selective COX-2 inhibitor **8a**. Compound **8a** (LM-1685) was selected as a promising candidate for further pharmacological evaluation.

Introduction

Nonsteroidal antiinflammatory drugs (NSAIDs) are useful tools in the treatment of inflammation, pain, and fever, although they show undesirable gastric side effects. Because NSAIDs directly target cyclooxygenases (COXs),¹ the discovery of the COX-2 isoform² has opened the possibility of developing COX-2 selective inhibitors to act as an effective NSAID without the gastric side effects.³ At present, two COX-2 selective inhibitors have successfully reached the market, Celecoxib⁴ (**1**) and Rofecoxib⁵ (**3**; see Chart 1), inducing a great interest in obtaining isozyme-specific drugs.⁶

To our knowledge, several attempts to derive COX-2 selective inhibitors from nonselective arylalkanoate NSAIDs have been published. Black et al. have described the obtention of COX-2 selective indolealkanoates emerging from indomethacin (**6**).⁷ Meanwhile,

Chart 1. Reference Compounds 1–7



Luong et al. preferred the basic framework of zomepirac to obtain pyrroleacetate selective inhibitors⁸ and Bayly et al. focused on flurbiprofen (**7**) to obtain selective inhibitors having the biphenylalkanoate framework.⁹ On the other hand, Kalgutkar et al. have recently described a general, biochemically based strategy for the

* To whom correspondence should be addressed. Present address: CIDF, Ferrer International S.A., Juan de Sada 32, 08028 Barcelona, Spain. Phone: +34-93-5093266. Fax: +34-93-4112764. E-mail: apalomer-research@ferrergrupo.com.

[†] Laboratorios Menarini S.A.

[‡] Universidad de Granada.

[§] Present address: Preclinical Pharmacology, Vita-Invest S.A., Av. Barcelona 69, 08970 Sant Joan Despí, Barcelona, Spain. Phone: +34-93-6022425. Fax: +34-93-3738351. E-mail: fcabre@vita-invest.com.

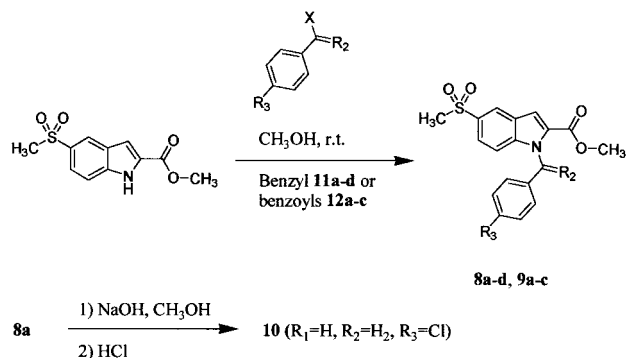
facile obtention of COX-2 selective molecules from carboxylic acid NSAIDs.¹⁰ In this approach, the compounds presumably exploit the constrictions at the base of the active site and a wide "lobby" present in the membrane-binding domain of the COX enzymes.¹¹ These results are consistent with the crystal structure of a complex of COX-2 with a carboxyl chain-extended analogue of zomepirac,⁸ as well as with the models describing the cavity at the mouth of the active site on the membrane-binding domain region of the COX enzymes.^{12,13} All these strategies focus on the modification of the carboxylic acid moiety or the distal phenyl ring not directly linked to the alkanolic acid, and the desired selectivity is introduced by systematic structural modification of the lead NSAIDs. Alternatively, selectivity may be introduced using the information presently available on the tricyclic COX-2 selective inhibitors structurally related to Celecoxib (**1**) and Rofecoxib (**3**).

The cyclooxygenase 3D structure has been known since the first X-ray crystal structure described by Picot et al.¹³ of the isoenzyme COX-1 complexed with the nonselective NSAID flurbiprofen (**7**). The structure of the human COX-2 enzyme, obtained from X-ray crystals¹⁴ or by homology modeling,¹⁵ has also been published. Kurumbail et al.¹⁶ have recently deposited in the Brookhaven Protein Databank structures of the COX-2 in free form as well as complexed with the selective inhibitor SC-558 (**2**) or the nonselective inhibitors indomethacin (**6**) and flurbiprofen (**7**). These structures have been used as the starting point for the present study.

Marriott et al. defined the pharmacophore as "an important and unifying concept in rational drug design that embodies the notion that molecules are active at a particular enzyme or receptor because they possess a number of chemical features (i.e., functional groups) that favorably interact with the target and which possess geometry complementary to it".¹⁷ It is possible to derive pharmacophores by direct analysis of the structure of a known ligand either in the most stable conformer or in the form observed when complexed with the target protein. For a derived pharmacophore model there are, in general, two ways to identify molecules that share its features and may thus elicit the desired biological response. First, there is the "3D database searching", where large databases comprising 3D structures are searched for those that match the pharmacophoric pattern.¹⁸ The second is de novo design that seeks to link the disjointed parts of the pharmacophore together with fragments in order to generate hypothetical structures.¹⁹ Typically, when used alone, de novo design produces wholly novel molecules but fails to identify chemical structures readily available or having a known synthesis. In contrast, when used in conjunction with a known chemical structure, i.e., modification of a known skeleton, it may successfully produce reasonably available products.

In this paper we detail our strategy to obtain selective COX-2 inhibitors based on the modification of the structure of the known potent but nonselective COX inhibitor indomethacin (**6**). The strategy intends to obtain selectivity using the information available on the tricyclic COX-2 selective inhibitors having the characteristic arylsulfonyl group believed to play a crucial role

Scheme 1. Synthesis of **8–10**



on the selectivity. With this aim, we applied a computer-assisted methodology based on the construction of a pharmacophore from the 3D structure of four known COX-2 selective inhibitors of the tricyclic class (**2–5**; see Chart 1) together with the knowledge of the X-ray crystal structure of COX-2 complexed with SC-558 (**2**). The application of the resulting pharmacophore to the design of indomethacin analogues having the basic indole framework allowed us to identify a small set of simple, novel COX-2 selective inhibitors structurally related to indomethacin (**6**).

Chemical Synthesis

Easy access to compounds of general structure **8a–d** and **9a–c** was made possible by the method of Ottoni et al.²⁰ As shown in Scheme 1, alkylation of the nitrogen atom of the commercially available methyl (5-methylsulfonyl-1H-2-indolyl)carboxylate (Acros Organics) afforded the benzyl derivatives **8a–d** in medium to good yields. Purified yields ranged from 57% (**8a**) to 95% (**8b** and **8d**). The same reaction using 4-substituted benzoyl chlorides led to derivatives **9a–c** in very poor yields but in sufficient quantities to carry out the biological assays. In the case of the *p*-chlorobenzoylation of **8a**, the nucleophilicity of the indole nitrogen atom was enhanced by converting the methyl (5-methylsulfonyl-1H-2-indolyl)carboxylate to the corresponding anion²¹ with NaH in DMF and the yield of **8a** was increased from 10% (KOH/MeOH) to 53%. Saponification of **8a** at room temperature gave **10** (57%).

Results and Discussion

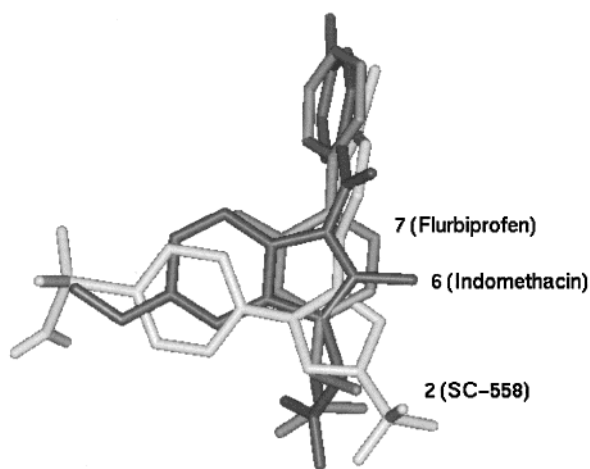
We used pharmacophore generation based on the structure of the known selective inhibitors and on the 3D structure of COX-2 inhibitor complexes, followed by ligand design and screening of compounds structurally related to indomethacin (**6**) to identify novel selective COX-2 inhibitors. The pharmacophore model was derived from the analysis of the selective inhibitors **2–5** (see Chart 1) in their most stable conformation and the structure of COX-2 complexed with SC-558 (**2**) or with the nonselective inhibitors indomethacin (**6**) and flurbiprofen (**7**) (protein database (pdb) entries 6cox, 4cox, and 3pgh, respectively).

Among all efforts to develop COX-2-selective inhibitors, the most successful strategies focus on the modification of structures of the tricyclic sulfonyl series leading to the marketed compounds Celecoxib (**1**) and Rofecoxib (**3**). These compounds differ significantly from the arylalkanoate structure of most NSAIDs, a marked

Table 1. Interactions with the Pharmacophore and Dihedral Angles between the Two Aromatic Ring Planes, Showing Summary of the Results Obtained for the Reference Compounds **2–6**

compd	Φ_{AB} (min energy conf) ^a (deg)	fit ^b	conf energy ^c (kcal mol ⁻¹)	mapping (conf no.) ^d	Φ_{AB} (mapping conf) ^e (deg)
2 (SC-558)	300 ^f	2.6	1.06	2 (24)	286
3 (Rofecoxib)	300	2.74	1.03	1 (23)	297
4 (DFU)	293	1.26	6.84	7 (4)	293
5	285	2.31	8.73	1 (9)	292
6 (indomethacin)	280 ^g	1.93	2.96	1 (1)	287

^a Φ_{AB} corresponds to the dihedral angle (deg) between the aromatic ring planes A and B in the minimum energy conformation obtained with the Catalyst modeling tools. ^b Values reported for the “fit” function are generated by Catalyst and reflect the number of features of the compounds and how well these features map onto the pharmacophore. ^c Values of “conformational energy” correspond to the energy, referenced to the energy of the most stable conformer, of the conformation that best maps the pharmacophore obtained with the Catalyst fitting tools. ^d Selected mapping and, in parentheses, the conformer number used in this mapping. ^e Dihedral angle between the aromatic ring planes A and B in the conformer that best maps the pharmacophore. ^f In the crystal structure of the COX-2 complexed with **2**, a dihedral angle between the two phenyl ring planes A and B of 273° is observed. ^g Indomethacin (**6**) lacks the characteristic S atom. Therefore, the described Φ_{AB} value corresponds to the dihedral angle between the indole and the phenyl ring planes of **6** observed in the crystal structure of the COX-2 complex.

**Figure 1.** Overlay of the crystal structures of COX-2 complexed with SC-558 (**2**), indomethacin (**6**), and flurbiprofen (**7**). Note in this overlay the superimposition of the aromatic ring planes (planes A and B in the pharmacophore).

difference being the presence of the sulfonyl group believed to be crucial for COX-1/COX-2 selectivity. Accordingly, this characteristic sulfur atom feature (sulfonyl sulfur atom) was the starting point for deriving the pharmacophore aimed at identifying novel COX-2 selective inhibitors. To outline other common chemical features that may be important for COX-2 inhibition, the alignments produced by the overlay of the crystal structures of COX-2 complexed with **2**, **6**, and **7** were analyzed (see Figure 1). Some interesting features can be deduced from this analysis: (i) the aromatic rings directly linked to the alkanate or sulfonyl groups lay in a common plane; (ii) the aromatic rings distant from the alkanate or sulfonyl groups also lay in a common plane; (iii) a common dihedral angle between both planes is observed for the three compounds analyzed. The pharmacophore model reflects these observations presenting the two cited aromatic ring planes A and B in a defined geometry and fixed position, i.e., a constrained dihedral angle between the ring planes and the normal to plane A in a confined position, respectively. Finally, an additional pharmacophoric feature was derived from the observation of the 3D crystallographic structure of the COX-2 complexes. The active site of COX-2 offers more accessible space than that of COX-1. This is due principally to the substitution of valine for isoleucine at position 523, which opens up a small

side pocket in COX-2. This additional space has proven to be important in the binding of some COX-2-selective inhibitors but imposes strict steric requirements by the enzyme for the ligands occupying in the proximity of amino acid 523. To include information about this region sterically forbidden to the ligands in our structure-based pharmacophore, we introduced an excluded volume feature centered in the valine 523 side chain γ position corresponding to the limits of the space available in COX-2.

The coordinates and geometry of the final pharmacophore model were derived from the structures of selective inhibitors **2–5** together with the 3D structure of COX-2 complexed with **2**. The conformational analysis and pharmacophore generation tools in the program Catalyst²² were used together with the available library of chemical descriptors. Coordinates of the S atom and the aromatic features (centroids of aromatic rings A and B) were obtained from the analysis of **2–5** in their most stable conformation. These conformers were also used to generate a valid geometric arrangement of the selected chemical functions. Thus, the dihedral angle between the cited planes in **2–5** was observed to lie between 280° and 300° (see Table 1) and was set to 290° \pm 10° in the pharmacophore. Similarly, a vector orthogonal to the aromatic ring plane A was defined (normal to plane A) and constrained to a defined position (additional globe situated at 3 Å from the ring A centroid; see Figure 2). The combined geometry of the dihedral angle and the position of the ring plane confine the configuration of these features and of the whole pharmacophore. As discussed above, in addition to pharmacophoric points derived from ligand atoms, an excluded volume that the ligand is not allowed to penetrate was centered in the valine 523 side chain γ position; the atomic coordinates were obtained from the 3D crystallographic structure of COX-2 complexed with **2** (see Figure 2).

A summary of the resulting chemical and geometrical features of the final pharmacophore model is shown in Table 2 and Figure 2. The performance of such a pharmacophore model was first evaluated by fitting the reference compounds **2** and **3** and the restrained analogues **5** (DFU) and **4**, using the rigid fit algorithm implemented in Catalyst. Rigid fit operations include an initial conformational exploration, followed by mapping of the chemical functionalities of each molecule in the pharmacophore by superimposing equivalent func-

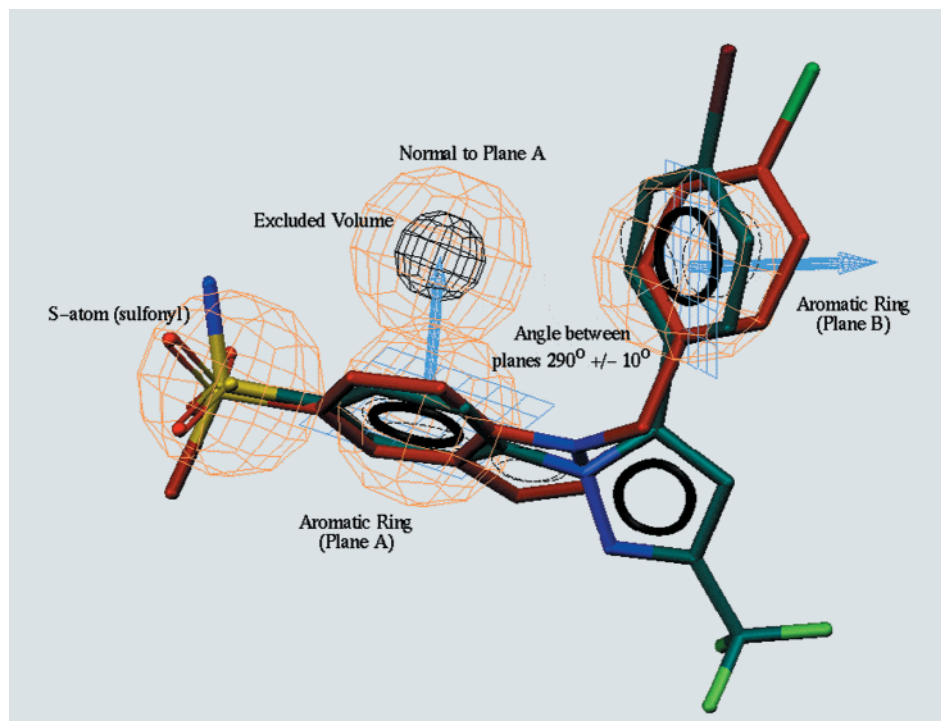


Figure 2. Pharmacophore with **2** (blue) and the modeled structure **A** (red) fitted. The pharmacophore contains a sulfonyl S atom (S), an aromatic ring feature (plane A) with a fixed position normal to the plane (labeled "Normal to Plane A"), an additional aromatic ring (plane B), both planes forming a dihedral angle of $290^\circ \pm 10^\circ$, and an excluded volume (labeled "Excluded Volume") accounting for the space limits imposed by residue 523. The chemical features are drawn as brown globes except for the hydrophobic aromatic ring plane A with an additional globe accounting for the position orthogonal to the plane and the excluded volume (black globe).

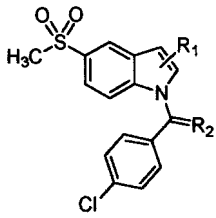
Table 2. Chemical Features Present in the Final Pharmacophore Model

	pharmacophore chemical and geometric features
sulfonyl S atom	characteristic of the phenylsulfonyl tricyclic series of compounds
aromatic ring A	
normal to plane A	constrained position of the normal to the ring plane A
aromatic ring A	constrained dihedral angle between planes A and B, $\Phi_{AB} = 290^\circ \pm 10^\circ$
excluded volume	accounts for the space limits imposed by the nonconserved residue 523

tional groups without modifying the geometry of the molecule (rigid fit operation). The program produces several maps per molecule as a result of this operation, together with the value of the "fit" function and the "conformational energy" for each proposed alignment. The "fit" value reflects the number of features of the compound and how well the features map onto the pharmacophore. Meanwhile, the "conformational energy" value reflects the energy of the selected conformer, referenced to the energy of the most stable conformation. The final step of the rigid fit operation consists of the selection of the most suitable molecule alignment, taking into account the "fit" values together with a visual inspection of the molecule overlay. Results are summarized in Table 1 with the outcome of the "fit" function and the "conformational energy" reported for the selected mappings of molecules **2–5**. Compounds **2** and **3**, and interestingly also the restrained analogues **4** and **5**, are able to effectively satisfy the proposed pharmacophore geometry with Φ_{AB} of about 290° , using energy accessible conformations ($E_{conf} < 10$ kcal/mol).

In general, the value of pharmacophore models is demonstrated by their ability to direct the obtention of novel compounds with the desired activity. Utility may be enhanced if the identified chemical structures are readily available or have a known synthesis. In the

present study, we evaluated the performance of the model by the identification of the selective COX-2 inhibitors arising from the pharmacophore model and the alignment of the crystallographic structures. Figure 1 illustrates that the *N*-benzoylindole skeleton of indomethacin (**6**) may be a suitable frame for obtaining COX-2 selectivity, and Table 1 shows that, despite the absence of the sulfur chemical feature, indomethacin (**6**) is able to reasonably map the pharmacophoric model. Accordingly, the structures **A–D**, related to indomethacin but possessing the additional sulfur group in the 5 position of the indole ring, were modeled and their ability to map the pharmacophore was evaluated. From the results summarized in Table 3, it can be deduced that, similar to their parent compounds **2–6**, the modeled structures **A–D** use energy accessible conformations to produce reasonable pharmacophoric maps. The successful application of the models stimulated us to further study compounds **8** and **9** derived from the modeled structures **A–D** (see Tables 3 and 4). A final modeling step was performed to construct the minimized complexes of COX-2 with **8a** and **9a**, structurally derived from **A–D** and further proposed for synthesis (see Table 4). The conformer alignments resulting from the pharmacophore mapping of the structures **A** and **D** were used as a guide to produce initial positions of **8a**

Table 3. Interactions with the Pharmacophore and Dihedral Angles between the Aromatic Ring Planes A and B, Showing Summary of the Results Obtained for the Modeled Structures A–D


compd	R ₁	R ₂	fit ^a	conf energy ^b (kcal mol ⁻¹)	mapping (conf no.) ^c	Φ _{AB} ^d
A	H	H ₂	2.73	1.88	2 (26)	291
B	2-CH ₃	H ₂	2.19	10.8	2 (23)	290
C	3-CH ₃	H ₂	2.89	3.94	1 (7)	295
D	H	=O	2.23	4.25	1 (21)	280

^a Values reported for the “fit” function are generated by Catalyst and reflect the number of features of the compounds and how well these features map onto the pharmacophore. ^b Values of “conformational energy” correspond to the energy, referenced to the energy of the most stable conformer, of the conformation that best maps the pharmacophore obtained with the Catalyst fitting tools. ^c Selected mapping and, in parentheses, the conformer number used in this mapping. ^d Dihedral angle between the indole and the phenyl ring planes (A and B) in the selected conformer mapping the pharmacophore.

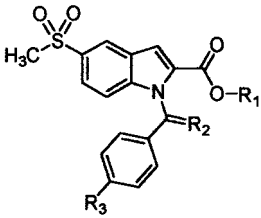
and **9a**, respectively. Then, the compounds were manually docked into the active site of COX-2 in a position that overlays **2**, and the geometry of the resulting complexes was optimized. Figure 3 shows the complex of the selective compound **8a** docked into the active site of COX-2. The final models illustrate the utility of the *N*-benzoylindole skeleton of indomethacin (**6**) suitable for obtaining COX-2 selectivity.

The successful modeling results obtained with the structures A–D prompted us to synthesize molecules **8–10**, having the basic *N*-benzyl- or *N*-benzoyl-5-sulfonylindole framework present in A–D, and to test them for COX inhibitory activity. Our in vitro screening scheme included the inhibition of the PGE₂ generation

**Figure 3.** Overlay of the modeled complexes of **8a** (colored by atom) and **2** (yellow) docked into the active site of COX-2. Note the superimposition of the pharmacophore chemical features (S atom, aromatic rings A and B and excluded volume) observed in this overlay.

in LPS-stimulated human monocytes (COX-2 cell assay) and the inhibition of the arachidonic acid (1 μM) induced TxB₂ generation in isolated human platelets (COX-1 cell assay). Furthermore, the selectivity of the compounds most effectively inhibiting COX-2 was established in the human in vitro whole blood assay.

In the set of cell-based in vitro tests, compounds **8a** (methyl [5-methylsulfonyl-1-(4-chlorobenzyl)-1*H*-2-indolyl]carboxylate; IC₅₀^{COX-2} = 0.65 ± 0.26 μM), **8d** (methyl [5-methylsulfonyl-1-(4-methoxybenzyl)-1*H*-2-indolyl]carboxylate; IC₅₀^{COX-2} = 0.78 ± 0.58 μM), and **9a** (methyl [5-methylsulfonyl-1-(4-chlorobenzoyl)-1*H*-2-indolyl]carboxylate; IC₅₀^{COX-2} = 0.73 ± 0.09 μM) demonstrated inhibition of the COX-2 activity with hardly any

Table 4. Chemical Structure of Compounds **8–10** and in Vitro COX-1 and COX-2 Activities


compd	benzoyl or benzyl ^a	R ₁	R ₂	R ₃	COX-2 ^{b,c} (IC ₅₀ , μM)	COX-1 ^d (% inhibition @ 10 μM)
8a	11a	CH ₃	H ₂	Cl	0.65 ± 0.26	19
8b	11b	CH ₃	H ₂	Br	3.72 ± 4.16	25
8c	11c	CH ₃	H ₂	NO ₂	> 20	0
8d	11d	CH ₃	H ₂	OCH ₃	0.78 ± 0.58	15
9a	12a	CH ₃	=O	Cl	0.73 ± 0.09	16
9b	12b	CH ₃	=O	Br	> 20	15
9c	12c	CH ₃	=O	NO ₂	> 20	n.t.
10		H	H ₂	Cl	> 20	37
1 (Celecoxib)					0.12 ± 0.04	IC ₅₀ = 2 ^c
3 (Rofecoxib)					0.21 ± 0.11	IC ₅₀ > 10 ^c
6 (indomethacin)					0.0059 ± 0.0005	IC ₅₀ = 0.0030 ± 0.002 ^c

^a See Scheme 1. ^b PGE₂ generation by LPS-stimulated human monocytes. ^c Dose–response curves were analyzed by nonlinear regression using the Hill equation as implemented in the GraphPad software Prism,³² and the IC₅₀ values were the concentration of the drug producing 50% cyclooxygenase inhibition. Values are the mean ± SD of at least three independent determinations. ^d % inhibition produced by tested compounds (10 μM concentration) on human platelets TxB₂ generation in the presence of 1 μM arachidonic acid.

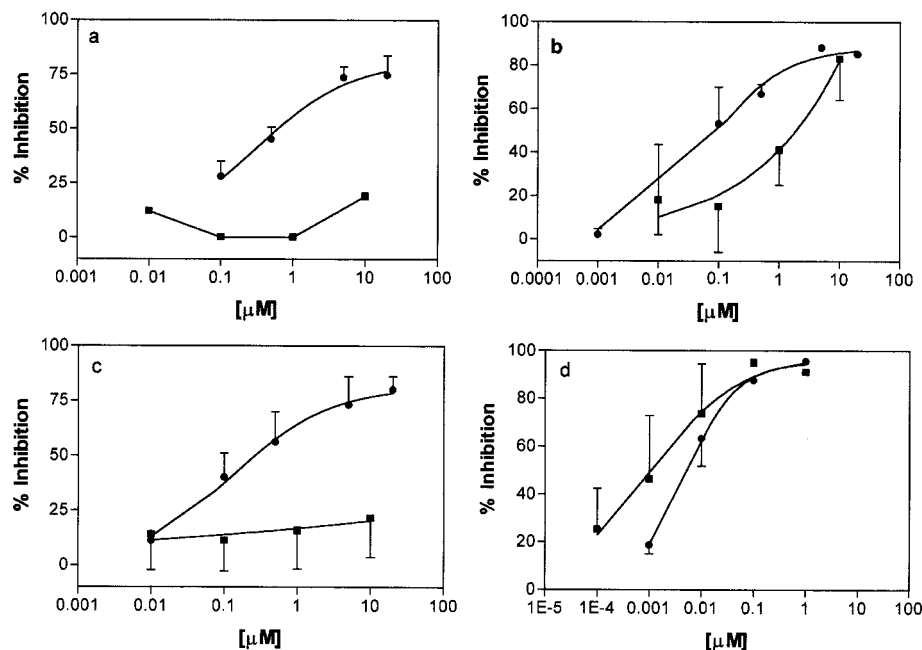


Figure 4. In vitro intact cell inhibition of COX-1 (■) and COX-2 (●) by **8a** (plot a) and the reference compounds Celecoxib (**1**; plot b), Rofecoxib (**3**; plot c), and indomethacin (**6**; plot d) (see also Table 4). The data shown are the mean of at least two experiments with the vertical lines indicating the standard deviation. The lines drawn through the data points are the result of fitting them to the Hill equation (for details, see footnote c in Table 4).

effect on COX-1 ($IC_{50}^{COX-1} \gg 10 \mu M$; see Table 4 and Figure 4). In addition, both series of *N*-benzyl and *N*-benzoyl compounds exemplified by **8** and **9** produced consistent structure–activity relationships. Thus, both series produced parallel inhibition (compare **8a–c** to **9a–c**, respectively, in Table 4) in accordance with the results obtained for the modeled structures **A** and **D**. Meanwhile, not all the assayed compounds that satisfy the pharmacophore features showed inhibition of the COX-2; i.e., the *N*-benzyl or *N*-benzoyl-5-sulfonylindole compounds having an additional nitro (**8c** and **9c**) or carboxylic acid groups (**10**) showed no production of cyclooxygenase inhibition ($IC_{50}^{COX-2} > 20 \mu M$). These results are in agreement with the general knowledge of COX inhibition²³ as well as with the pharmacophore concept. The latter embodies the notion that molecules are active at a particular receptor because they possess the adequate ensemble of chemical features in a defined geometric disposition complementary with the receptor. However, the pharmacophore may reflect an incomplete picture of the interactions with the receptor or, most frequently, may not account for features that cause the activity to plummet. In this sense, the inactivity of **10** may arise from the unfavorable simultaneous presence of a carboxylic acid and a sulfonyl group in the molecule, a fact that is known to decrease activity. Meanwhile, the inactivity of **8c** and **9c** may be due to the substitution with the polar NO_2 group in the phenyl oriented toward the hydrophobic gap near Trp-386 and Tyr-385. Certainly, such chemical features unfavorable for activity are not present in the pharmacophore.

The selectivity of the most effective compounds as far as COX-2 inhibition is concerned (**8a**, **8d**, and **9a**) was established using the human whole blood assay (results are summarized in Table 5). In this suite of assays, **8a** showed interesting COX-2 inhibition results. Meanwhile, **8d** and **9a** were found to be more discrete.

Table 5. Inhibitory Effect on COX-2 and COX-1 Activities Determined in Human Whole Blood

compd	COX-2 ^a (IC_{50} , μM)	COX-1 ^b (% inhibition @ 100 μM)	COX-1/COX-2
8a	4.3 ± 0.3	25	>20
8d	51.3 ± 9.1	54	2
9a	<25% at 10 μM not tested		
1 (Celecoxib)	3.6 ± 1.2	$IC_{50} = 26.4 \pm 12.7$	7.3
3 (Rofecoxib)	3.4 ± 2.3	$IC_{50} = 28.7 \pm 13.1$	8.4
6 (indomethacin)	0.63 ± 0.08	$IC_{50} = 0.23 \pm 0.12^b$	0.37

^a COX-2 activity was evaluated in human whole blood as LPS-induced PGE₂ generation. IC_{50} values were estimated from dose–response curves analyzed by nonlinear regression using the Hill equation as implemented in the GraphPad software Prism³² and mean the concentration of the drug causing 50% reduction of cyclooxygenase activity measured in the absence of compound. IC_{50} values are the mean \pm SD of at least three independent determinations. ^b % inhibition produced by tested compounds at 100 μM concentration on TxB₂ production by human whole blood according to the procedures described in the Experimental Section.

Compound **8a** was almost 1 order of magnitude more potent than **8d**. In addition, **8a** inhibited COX-2 in a similar range as the reference compounds Celecoxib (**1**) and Rofecoxib (**3**) ($IC_{50}^{COX-2} = 4.3 \pm 0.3$, 3.6 ± 1.2 , and 3.4 ± 2.3 , respectively), and more interestingly, **8a** showed a clearly favorable COX-1/COX-2 ratio compared to the same reference compounds ($IC_{50}^{COX-1}/IC_{50}^{COX-2} = >20$, 7.3, and 8.4, respectively).

The strategy followed in the present study to obtain the pharmacophore model was based on the use of the available information on the tricyclic COX-2 selective inhibitors related to Celecoxib (**1**) and Rofecoxib (**3**); therefore, the resulting selectivity is derived from the use of this structural information rather than the systematic modification of the arylalkanoate framework of the NSAID indomethacin (**6**). Moreover, aside from its COX-2 inhibitory potency and selectivity, **8** and **9** are simple structures with limited similarity to existing

selective COX-2 inhibitors, and their physical properties, such as molecular weight and log *P*, are presumably within the range expected for good drugs. This latter is reinforced by the interesting anti-COX-2 activity obtained for **8a** in the in vitro human whole blood assay.

Conclusions

In the present work we describe the obtention of selective COX-2 inhibitors evolved from the known potent nonselective COX inhibitor indomethacin (**6**). Our computer-aided strategy is based on the construction of a pharmacophore model from the 3D structure of four COX-2 selective inhibitors of the tricyclic class together with the knowledge of the X-ray crystal structures of COX-2 complexed with inhibitors. The compounds used for pharmacophore development were SC-558 (**2**; structural analogue of Celecoxib (**1**)) and Rofecoxib (**3**) together with the restrained analogues **5** (DFU) and **4**. Meanwhile, we used the 3D crystal structures of COX-2 complexed with the selective inhibitor SC-558 (**2**) and the nonselective NSAIDs indomethacin (**6**) and flurbiprofen (**7**). The resulting pharmacophore was then applied to the design of indomethacin analogues having the basic *N*-benzyl- or *N*-benzoyl-5-sulfonylindole framework exemplified by the modeled structures **A–D**. Finally, the synthesis of compounds **8–10** allowed us to identify the compounds **8a**, **8d**, and **9a** as being potent inhibitors of the COX-2 from human monocytes ($IC_{50}^{COX-2} = 0.65, 0.78, \text{ and } 0.73 \mu\text{M}$, respectively) with hardly any effect on the COX-1 from human platelets ($IC_{50}^{COX-1} \gg 10 \mu\text{M}$). After the inhibitory effect and selectivity of these compounds in whole blood were analyzed, **8a** was confirmed as a promising candidate for further evaluation.

Experimental Section

1. Chemistry. All solvents were used dried and freshly distilled. All evaporations were carried out in vacuo with a rotary evaporator. Solutions were dried over MgSO_4 before concentration under reduced pressure. Analytical samples were normally dried in vacuo over P_2O_5 at 40–50 °C for 16 h. Analytical thin-layer chromatography (TLC) was done on Merck silicagel F-254 plates with detection with iodine and a UV lamp or by charring with dilute sulfuric acid, using mixtures of $\text{CH}_2\text{Cl}_2/\text{MeOH}$ (10:0.1) as the developing solvent. All analytical samples were TLC homogeneous. For normal column chromatography Merck silica gel 60 was used with a particle size of 0.063–0.200 mm (70–230 mesh ASTM). For flash chromatography Merck silica gel 60 was used with a particle size of 0.040–0.063 mm (230–400 mesh ASTM). Melting points (mp) were obtained on an Electrothermal melting point apparatus and are uncorrected. NMR spectra were recorded on 400.1 MHz ^1H and 100.03 MHz ^{13}C NMR Bruker ARX 400 and 300.13 MHz ^1H and 75.78 MHz ^{13}C NMR Bruker AM-300 spectrometers, and chemical shifts are reported relative to the solvent peak. Chemical shifts (δ) quoted in the case of multiplets were measured from the approximate center. Signals are designated as follows: s, singlet; d, doublet; dd, doublet of doublets; m, multiplet. Coupling constants are expressed in hertz. High-resolution liquid secondary ion mass spectra (HR LSIMS) were carried out on a VG AutoSpec Q high-resolution mass spectrometer (Fisons Instruments). The compounds gave accurate mass spectra, having no extraneous peaks. All products had satisfactory (within $\pm 0.4\%$ of the theoretical values) C, H, and N analyses results. The yields reported are of the isolated purified compounds and are not optimized for **9b** and **9c**.

General Procedure for the Preparation of Methyl [5-Methylsulfonyl-1-(4-substituted benzyl)-1*H*-2-indolyl]carboxylate (8a–d**) and Methyl [5-Methylsulfonyl-1-(4-substituted benzoyl)-1*H*-2-indolyl]carboxylate (**9a–c**).** To a solution of methyl (5-methylsulfonyl-1*H*-2-indolyl)carboxylate (2.2 mmol) in methanol (20 mL) at room temperature, KOH pellets were added (2.7 mmol), and the mixture was stirred until total solubilization was attained. The methanol was completely removed in vacuo, and acetone (20 mL) was added followed by the 4-substituted benzyl bromide (**11a–d**) (2.2 mmol) or the 4-substituted benzoyl chloride (**12a–c**) (2.2 mmol). The mixture was left overnight, concentrated in a vacuum, and purified by flash chromatography, yielding **8a–d** or **9a–c** as white solids.

Methyl [5-methylsulfonyl-1-(4-chlorobenzyl)-1*H*-2-indolyl]carboxylate (8a**):** yield 57%; mp 177–179 °C; ^1H NMR (300.13 MHz, $\text{DMSO}-d_6$) δ 8.38 (s, 1H, H-4), 7.84 (d, $J = 8.9$ Hz, 1H, H-7), 7.80 (dd, $J_1 = 8.9, J_2 = 1.6$ Hz, 1H, H-6), 7.60 (s, 1H, H-3), 7.32 (d, $J = 8.5$ Hz, 2H, benzyl), 7.03 (d, $J = 8.5$ Hz, 2H, benzyl), 5.80 (s, 2H, $\text{N}-\text{CH}_2-$), 3.83 (s, 3H, $\text{CH}_3\text{O}-$), 3.19 (s, 3H, CH_3SO_2-); ^{13}C NMR (75.78 MHz, $\text{DMSO}-d_6$) δ 161.09 (C=O), 140.09, 136.81, 133.56, 131.81, 129.22, 128.52, 128.10, 124.79, 123.21, 123.01, 112.27, 112.20, 52.10 ($\text{CH}_3\text{O}-$), 46.92 ($\text{N}-\text{CH}_2-$), 44.07 (CH_3SO_2-); HR LSIMS calcd for $\text{C}_{18}\text{H}_{16}\text{O}_4\text{NaNSCl}$ [$\text{M} + \text{Na}$] $^+$ 400.0386, found 400.0386. Anal. ($\text{C}_{18}\text{H}_{16}\text{O}_4\text{NaNSCl}$) C, H, N.

Methyl [5-methylsulfonyl-1-(4-bromobenzyl)-1*H*-2-indolyl]carboxylate (8b**):** yield 95%; mp 185–189 °C; ^1H NMR (400.13 MHz, CDCl_3) δ 8.37 (d, $J = 1.7$ Hz, 1H, H-4), 7.81 (dd, $J_1 = 8.9, J_2 = 1.7$ Hz, 1H, H-6), 7.49 (d, $J = 0.7$ Hz, 1H, H-3), 7.46 (d, $J = 8.9$ Hz, 1H, H-7), 7.37 (d, $J = 8.5$ Hz, 2H, benzyl), 6.09 (d, $J = 8.5$ Hz, 2H, benzyl), 5.82 (s, 2H, $\text{N}-\text{CH}_2-$), 3.89 (s, 3H, $\text{CH}_3\text{O}-$), 3.07 (s, 3H, CH_3SO_2-); ^{13}C NMR (100.03 MHz, CDCl_3) δ 161.72 (C=O), 141.11, 136.24, 133.36, 131.98, 129.89, 128.05, 125.62, 124.12, 123.40, 121.58, 112.46, 111.70, 52.26 ($\text{CH}_3\text{O}-$), 47.83 ($\text{N}-\text{CH}_2-$), 45.08 (CH_3SO_2-); HR LSIMS calcd for $\text{C}_{18}\text{H}_{16}\text{O}_4\text{NaNSBr}$ [$\text{M} + \text{Na}$] $^+$ 443.9881, found 443.9881. Anal. ($\text{C}_{18}\text{H}_{16}\text{O}_4\text{NaNSBr}$) C, H, N.

Methyl [5-methylsulfonyl-1-(4-nitrobenzyl)-1*H*-2-indolyl]carboxylate (8c**):** yield 64%; mp 222–229 °C; ^1H NMR (300.13 MHz, $\text{DMSO}-d_6$) δ 9.23 (s, 1H, H-4), 8.96 (d, $J = 8.7$ Hz, 2H, benzyl), 8.65 (m, 2H, H-6, and H-7), 8.47 (s, 1H, H-3), 8.05 (d, $J = 8.7$ Hz, 2H, benzyl), 6.04 (s, 2H, $\text{N}-\text{CH}_2-$), 3.81 (s, 3H, $\text{CH}_3\text{O}-$), 3.20 (s, 3H, CH_3SO_2-); ^{13}C NMR (75.78 MHz, $\text{DMSO}-d_6$) δ 161.09 (C=O), 146.70, 145.77, 140.64, 133.77, 129.27, 127.27, 124.90, 123.86, 123.39, 123.28, 112.42, 112.24, 52.20 ($\text{CH}_3\text{O}-$), 47.36 ($\text{N}-\text{CH}_2-$), 44.09 (CH_3SO_2-). Anal. ($\text{C}_{18}\text{H}_{16}\text{O}_6\text{N}_2\text{S}\cdot 0.5\text{H}_2\text{O}$) C, H, N.

Methyl [5-methylsulfonyl-1-(4-methoxybenzyl)-1*H*-2-indolyl]carboxylate (8d**):** yield 95%; mp 157–162 °C; ^1H NMR (400.13 MHz, $\text{DMSO}-d_6$) δ 8.35 (d, $J = 1.7$ Hz, 1H, H-4), 7.87 (d, $J = 8.9$ Hz, 1H, H-7), 7.79 (dd, $J_1 = 8.9, J_2 = 1.7$ Hz, 1H, H-6), 7.58 (s, 1H, H-3), 7.02 (d, $J = 8.7$ Hz, 2H, benzyl), 6.81 (d, $J = 8.7$ Hz, 2H, benzyl), 5.83 (s, 2H, $\text{N}-\text{CH}_2-$), 3.85 (s, 3H, $\text{CH}_3\text{OCO}-$), 3.65 (s, 3H, 3.65 (s, 3H, $\text{CH}_3\text{O}-$), 3.18 (s, 3H, CH_3SO_2-); ^{13}C NMR (100.03 MHz, $\text{DMSO}-d_6$) δ 161.27 (C=O), 158.47, 140.47, 133.38, 129.68, 129.23, 127.86, 124.81, 123.22, 122.88, 113.97, 112.54, 112.13, 55.00 ($\text{CH}_3\text{O}-$), 52.16 ($\text{CH}_3\text{O}-$), 46.92 ($\text{N}-\text{CH}_2-$), 44.11 (CH_3SO_2-); HR LSIMS calcd for $\text{C}_{19}\text{H}_{19}\text{O}_5\text{NaNS}$ [$\text{M} + \text{Na}$] $^+$ 396.0882, found 396.0884. Anal. ($\text{C}_{19}\text{H}_{19}\text{O}_5\text{NS}$) C, H, N.

Methyl [5-methylsulfonyl-1-(4-chlorobenzoyl)-1*H*-2-indolyl]carboxylate (9a**):** yield 10%. This yield was improved to 53% using NaH to generate the indole anion: a solution of 2.5 g (8.8 mmol) of methyl (5-methylsulfonyl-1*H*-2-indolyl)carboxylate in DMF (15 mL) was stirred under an argon atmosphere with 224 mg of NaH (60% in mineral oil; 9.3 mmol) for 5 min and then with 1.64 g (9.3 mmol) of 4-chlorobenzoyl chloride (**11a**) for 1 h. The solution was diluted with water and extracted with EtOAc. The organic phase was washed with brine, dried, and concentrated. The residue was purified by flash chromatography ($\text{CH}_2\text{Cl}_2/\text{hexane}$, 1:3): mp 157–159 °C; ^1H NMR (300.13 MHz, CDCl_3) δ 8.36 (d, $J = 1.7$ Hz, 1H, H-4), 7.91 (dd, $J_1 = 8.9, J_2 = 1.7$ Hz, 1H, H-6), 7.83 (d, $J = 8.9$ Hz, 1H,

H-7), 7.61 (d, $J = 8.7$ Hz, 2H, benzyl), 7.46 (s, 1H, H-3), 7.45 (d, $J = 8.7$ Hz, 2H, benzyl), 3.64 (s, 3H, CH_3O-), 3.09 (s, 3H, CH_3SO_2-); ^{13}C NMR (75.78 MHz, $CDCl_3$) δ 167.67 ($-C=O$ ester), 160.63 ($C=O$), 140.66, 135.92, 132.99, 132.72, 130.78, 129.51, 127.03, 125.40, 123.53, 115.22, 114.75, 52.63 (CH_3O-), 44.99 (CH_3SO_2-); HR LSIMS calcd for $C_{18}H_{14}O_5NaNSCl$ [$M + Na$] $^+$ 414.0178, found 414.0180. Anal. ($C_{18}H_{14}O_5NSCl$) C, H, N.

Methyl [5-methylsulfonyl-1-(4-bromobenzoyl)-1H-2-indolyl]carboxylate (9b): yield 10%; mp 170–171 °C; 1H NMR (400.13 MHz, $CDCl_3$) δ 8.38 (d, $J = 1.7$ Hz, 1H, H-4), 7.93 (dd, $J_1 = 8.8$, $J_2 = 1.6$ Hz, 1H, H-6), 7.85 (d, $J = 8.8$, 1H, H-7), 7.64 (d, $J = 8.6$ Hz, 2H, benzyl), 7.55 (d, $J = 8.6$ Hz, 2H, benzyl), 7.48 (s, 1H, H-3), 3.65 (s, 3H, CH_3O-), 3.10 (s, 3H, CH_3SO_2-); ^{13}C NMR (100.03 MHz, $CDCl_3$) δ 167.86 ($-C=O$ ester), 160.63 ($C=O$), 140.63, 135.84, 133.42, 132.67, 132.50, 130.80, 129.31, 127.01, 125.43, 123.54, 115.30, 114.79, 52.68 (CH_3O-), 45.00 (CH_3SO_2-); HR LSIMS calcd for $C_{18}H_{14}O_5NaNSBr$ [$M + Na$] $^+$ 457.9674, found 457.9676. Anal. ($C_{18}H_{14}O_5NSBr$ ·0.1H₂O) C, H, N.

Methyl [5-methylsulfonyl-1-(4-nitrobenzoyl)-1H-2-indolyl]carboxylate (9c): yield 7.5%; mp 202–204 °C; 1H NMR (400.13 MHz, $CDCl_3$) δ 8.39 (d, $J = 1.4$ Hz, 1H, H-4), 8.31 (d, $J = 8.8$ Hz, 2H, benzyl), 8.01 (d, $J = 8.9$, 1H, H-7), 7.97 (dd, $J_1 = 8.9$, $J_2 = 1.4$ Hz, 1H, H-6), 7.81 (d, $J = 8.8$ Hz, 2H, benzyl), 7.52 (s, 1H, H-3), 3.61 (s, 3H, CH_3O-), 3.10 (s, 3H, CH_3SO_2-); ^{13}C NMR (100.03 MHz, $CDCl_3$) δ 167.00 ($-C=O$ ester), 160.46 ($C=O$), 150.47, 140.78, 140.15, 136.46, 132.21, 130.03, 126.03, 124.12, 123.64, 116.32, 115.03, 52.79 (CH_3O-), 44.95 (CH_3SO_2-). Anal. ($C_{18}H_{14}O_7N_2S$) C, H, N.

[5-Methylsulfonyl-1-(4-chlorobenzoyl)-1H-2-indolyl]carboxylic Acid (10). To a solution of **8a** (270 mg, 0.71 mmol) in MeOH (3 mL) was added a solution of NaOH (70 mg, 1.77 mmol) in H₂O (2 mL). The resulting solution was stirred for 10 h. After being cooled in an ice-bath, it was neutralized with concentrated HCl, rotaevaporated off, and purified by flash chromatography ($CH_2Cl_2/MeOH$, 10:0.6). Pure acid **10** was obtained (150 mg, 57%) as a white solid: mp 233–235 °C; 1H NMR (400.13 MHz, CD_3OD) δ 8.36 (d, $J = 1.7$ Hz, 1H, H-4), 7.80 (dd, $J_1 = 8.9$, $J_2 = 1.7$ Hz, 1H, H-6), 7.65 (d, $J = 8.9$, 1H, H-7), 7.55 (s, 1H, H-3), 7.23 (d, $J = 8.4$ Hz, 2H, benzyl), 7.02 (d, $J = 8.4$ Hz, 2H, benzyl), 5.93 (s, 2H, $N-CH_2-$), 3.11 (s, 3H, CH_3-); ^{13}C NMR (100.03 MHz, CD_3OD) δ 164.17 ($-C=O$), 142.52, 138.10, 134.46, 133.94, 132.19, 129.70, 129.13, 127.04, 124.73, 123.98, 113.35, 113.09, 48.36 ($N-CH_2-$), 44.94 (CH_3-); HR LSIMS calcd for $C_{17}H_{13}O_4Na_2NSCl$ [$M + 2Na - H$] $^+$ 408.0049, found 408.0049. Anal. ($C_{17}H_{14}O_4NSCl$) C, H, N.

2. Molecular Modeling. 2.a. General Methodology. All molecular modeling studies were performed on a Silicon Graphics O₂ computer running the Catalyst software (version 2.2) and the InsightII (version 97)²⁴ and Discover (version 2.98)²⁴ software (Molecular Simulations, Inc., San Diego, CA). The basic modeling methodologies leading to the pharmacophore-based alignments (e.g., conformational analysis, molecule fitting, etc.) were performed with Catalyst using the implemented chemical features²⁵ and the energy minimization procedure using a standard conjugate gradients minimization algorithm and a modified version of the CHARMM molecular mechanics force field.²⁶ The underlying operation of the Catalyst software has already been described in detail. Conformational analysis was performed as implemented in the program using the above-described minimizer coupled to a "poling" function to assess conformational variation²⁷ and the BEST algorithm, which intends to optimize the conformational coverage versus the size of the assembly.^{28,29} In the calculation, a threshold of 250 conformers per molecule and a maximum of 20 kcal/mol was used.

2.b. Catalyst Pharmacophore Construction and Molecule Mapping. The hypothesis generation was based on the analysis of **2–5** in their most stable conformation in order to identify common chemical features and valid geometric arrangement of these chemical functions to generate the pharmacophore model. The library of chemical descriptors in the program was used to map the chemical functionalities in

each molecule. The fitting of a molecule onto the pharmacophore was performed with Catalyst, taking into account the chemical features present in the molecule. Fitting operations were done using the FAST algorithm implemented in Catalyst, which do not alter the geometry of the molecule (rigid fit) and consist of the following steps: (1) conformational search as described above using the implemented force field and a poling function to ensure conformational diversity; (2) mapping of the chemical functionalities of each molecule by superimposing equivalent functional groups without modifying the geometry of the molecule (rigid fit operation); (3) selection of the most suitable alignment among the set of mappings proposed by Catalyst. The mapping operation in Catalyst produces several maps per molecule and reports, for each mapping, the values of the "fit" function and the "conformational energy". The "fit" value reflects the number of features of the compound and how well the features map onto the pharmacophore. Meanwhile, the "conformational energy" value reflects the energy of the selected conformer, referenced to the energy of the most stable conformation. The different maps per molecule produced by the Catalyst fit operation effectively satisfy the proposed pharmacophore geometry. Therefore, for relatively simple pharmacophores (less than or equal to four pharmacophoric points) some of the proposed alignments are irrelevant, and it is recommended that the overall superimposition onto the reference compounds be visually inspected. The final mapping was selected among the proposed alignments, taking into account the "fit" values together with a visual inspection of the overall superposition onto the reference compounds **2** and **3**. The values of the "fit" function and the "conformational energy" were reported for the selected mapping.

2.c. COX Inhibitor Complexes. The basic modeling methodologies leading to the energy-minimized complexes were performed using the cvff molecular mechanics force field implemented in Discover with a dielectric constant of 4 r and a 12 Å cutoff to compute the nonbonded interactions. Energy minimization was performed using the standard steepest descent and conjugate gradients minimization algorithms implemented in the program, leaving the complete structure free to relax. For consistency with most publications in the field, amino acid numbering throughout this work refers to the ovine COX-1 sequence.

3. Pharmacology. 3.a. TxB₂ Production by Human Platelets. COX-1 activity was evaluated as thromboxane B₂ (TxB₂) generation in human platelets as described elsewhere.³⁰ Washed human platelets were suspended in H.H. buffered solution (Hank's balanced salt solution containing 1 mM CaCl₂ and 0.5 mM MgCl₂, pH 7.4) at 8 × 10⁶ platelets/mL final concentration. A total of 400 μL of platelet suspension was preincubated for 15 min at 37 °C with a solvent or drug solution and then incubated for another 10 min with 1 μM arachidonic acid in a final volume of 1 mL. The reaction was stopped by the addition of 0.5 mL of 2% formic acid followed by centrifugation at 10 000 rpm for 2 min. Supernatants were stored at –80 °C until assayed for their content on TXB₂ using a competitive enzyme immunoassay.

3.b. PGE₂ Generation by LPS-Stimulated Human Monocytes. Induction and inhibition of COX-2 activity in human monocytes were conducted in accordance to previously reported procedures.³¹ Mononuclear cells were separated from buffy coats by Ficoll-Paque. After centrifugation (400g for 40 min at room temperature), lymphomonocytes were layered at the gradient interface while PMN were in the bottom fraction. Mononuclear cells were carefully removed, washed three times, and resuspended in Dulbecco's modified Eagle's medium (DMEM) buffered with 0.05 M HEPES, pH 7.4, supplemented with 0.5% heat-inactivated FCS and 4 mM l-glutamine. This will be referred to as a complete medium (CDMEM). Aliquots of 10 mL were seeded into plastic Petri dishes and incubated at 37 °C in 5% CO₂-humidified atmosphere for 60 min. The adherent cells were recovered by gently scraping with a rubber policeman and resuspended in CDMEM (3 × 10⁶ cells/mL), and their viability (>96%) was examined by trypan blue exclusion. The cell suspension was constituted of >90% mono-

cytes. Isolated monocytes were incubated in CDMEM for 24 h at 37 °C in 5% CO₂-humidified atmosphere in the absence and in the presence of LPS (10 µg/mL). The effect of inhibitors was studied by incubating the monocytes suspension with each drug at different concentrations in the presence of LPS. The supernatant was separated by centrifugation (10 min at 2000 rpm) and kept at -80 °C until it was assayed for PGE₂ by specific enzyme immunoassay. Blanks and vehicle controls were included in each experiment. All tests and controls were performed in triplicate.

3.c. COX-2 Activity in Human Whole Blood. Fresh blood was collected in heparinized tubes by venipuncture from volunteers with consent. The subjects had no apparent inflammatory conditions and had not taken any NSAID for at least 7 days prior to blood collection. A total of 10 mL of blood was mixed with 100 µL of LPS (1 mg/mL), and the mixture was gently stirred for 10 min. Aliquots of this mixture were incubated for 24 h at 37 °C with either vehicle (0.2% DMSO in saline as the final concentration) or test compound at different selected concentrations. Appropriate controls, blood incubated with only vehicle, were used as blanks. The incubation was interrupted by centrifugation. The supernatant, plasma, was divided into two aliquots and stored at -80 °C until analysis for PGE₂ levels using enzyme immunoassay.

3.d. COX-1 Activity in Human Whole Blood. Fresh blood was collected as described above. Aliquots were transferred to microcentrifuge tubes preloaded with either DMSO or the test compound at different selected concentrations. Mixtures were gently stirred for 40 min at 37 °C. Then calcium ionophore A23187 (final concentration of 25 µM) was added to all tubes except blanks, which received DMSO. Samples were vortexed and incubated 20 min more at 37 °C. The process was stopped by introducing the tube into an ice bath (4 °C) followed by centrifugation. As in the COX-2 assay, two aliquots of the supernatant were stored at -80 °C until TxB₂ analysis by means of enzyme immunoassay.

Acknowledgment. This work was financed in part by a grant from the Spanish Ministry of Education (CDTI), Grant No. 98-0413. The authors thank Dr. A. Giolitti (Menarini Ricerche S.p.A.) for helpful discussions and assistance in reviewing the manuscript.

References

- Flower, R. J.; Vane, J. R. Inhibition of Prostaglandin Synthetase in Brain Explains the Anti-pyretic Activity of Paracetamol (4-Acetamidophenol). *Nature* **1972**, *240*, 410–411.
- Xie, W.; Chipmann, J. G.; Robertson, D. L.; Erikson, R. L.; Simmons, D. L. Expression of a Mitogen-Responsive Gene Encoding Prostaglandin Synthase Is Regulated by mRNA Splicing. *Proc. Natl. Acad. Sci. U.S.A.* **1991**, *88*, 2692.
- Smith, W. L.; Garavito, R. M.; DeWitt, D. L. Prostaglandin Endoperoxide H Synthases (Cyclooxygenases)-1 and -2. *J. Biol. Chem.* **1996**, *271*, 33157–33160.
- Penning, T. D.; Talley, J. J.; Bertenshaw, S. R.; Carter, J. S.; Collins, P. W.; Docter, S.; Graneto, M. J.; Lee, L. F.; Malecha, J. W.; Miyashiro, J. M.; Rogers, R. S.; Rogier, D. J.; Yu, S. S.; Anderson, G. D.; Burton, E. G.; Cogburn, J. N.; Gregory, S. A.; Koboldt, C. M.; Perkins, W. E.; Seibert, K.; Veenhuizen, A. W.; Zhang, Y. Y.; Isakson, P. C. Synthesis and Biological Evaluation of the 1,5-Diarylpyrazole Class of Cyclooxygenase-2 Inhibitors: Identification of 4-[5-(4-Methylphenyl)-3-(trifluoromethyl)-1H-pyrazol-1-yl]benzene Sulfonamide (SC-58635, Celecoxib). *J. Med. Chem.* **1997**, *40* (9), 1347–1365.
- Ehrich, E.; Dallob, A.; van Hecken, A.; Depre, M.; DeLepeleire, I.; Brideau, C.; Hilliard, D.; Tanaka, W.; Mukhopadhyay, S.; Seibold, J.; DeSchepper, P.; Gertz, B. Demonstration of Selective COX-2 Inhibition by MK-966 in Humans. *Arthritis Rheum.* **1996**, *39* (9), s81 (Abstract 328).
- Hawkey, C. J. COX-2 Inhibitors. *Lancet* **1999**, *353*, 307–314.
- Black, W. C.; Bayly, C.; Belley, M.; Chan, C. C.; Charleson, S.; Denis, D.; Gauthier, J. Y.; Gordon, R.; Guay, D.; Kargman, S.; Lau, C. K.; Leblanc, Y.; Mancini, J.; Ouellet, M.; Percival, D.; Roy, P.; Skorey, K.; Tagari, P.; Vickers, P.; Wong, E.; Xu, L.; Prasit, P. From Indomethacin to a Selective COX-2 Inhibitor: Development of Indolalkanoic Acids as Potent and Selective Cyclooxygenase-2 Inhibitors. *Bioorg. Med. Chem. Lett.* **1996**, *6*, 725–730.
- Luong, C.; Miller, A.; Barnett, J.; Chow, J.; Ramesha, C.; Browner, M. F. Flexibility of the NSAID Binding Site in the Structure of Human Cyclooxygenase-2. *Nat. Struct. Biol.* **1996**, *3*, 927–933.
- Bayly, C. I.; Black, C.; Leger, S.; Ouimet, N.; Ouellet, M.; Percival, M. D. Structure-Based Design of COX-2 Selectivity into Flurbiprofen. *Bioorg. Med. Chem. Lett.* **1999**, *9*, 307–312.
- Kalutkar, A. S.; Crews, B. C.; Rowlinson, S. W.; Marnett, A. B.; Kozak, K. R.; Rimmel, R. P.; Marnett, L. J. Biochemically-Based Design of Cyclooxygenase-2 (COX-2) Inhibitors: Facile Conversion of Nonsteroidal Antiinflammatory Drugs to Potent and Highly Selective COX-2 Inhibitors. *Proc. Natl. Acad. Sci. U.S.A.* **2000**, *97*, 925–930.
- Kalutkar, A. S.; Marnett, A. B.; Crews, B. C.; Rimmel, R. P.; Marnett, L. J. Ester and Amide Derivatives of the Nonsteroidal Antiinflammatory Drug, Indomethacin, as Selective Cyclooxygenase-2 Inhibitors. *J. Med. Chem.* **2000**, *43*, 2860–2870.
- Llorens, O.; Perez, J. J.; Palomer, A.; Mauleón, D. Structural Basis of the Dynamic Mechanism of Ligand Binding to Cyclooxygenase. *Bioorg. Med. Chem. Lett.* **1999**, *9*, 2779–2784.
- Picot, D.; Loll, P. J.; Garavito, R. M. The X-ray Crystal Structure of the Membrane Protein Prostaglandin H₂ Synthase-1. *Nature* **1994**, *367*, 243–249.
- McKeever, B. M.; Pandya, S.; Percival, M. D.; Ouellet, M.; Bayly, C.; O'Neill, G. P.; Bastien, L.; Kennedy, B. P.; Adam, M.; Cromlish, W.; Roy, P.; Black, W. C.; Guay, D.; LeBlanc, Y. Crystal Structure of Recombinant Human COX-2 at 3.0 Å Resolution. *Conf. Prostaglandin Relat. Compd., 10th* **1996**, *55* (1), 20 (Abstract 63).
- Filizola, M.; Pérez, J. J.; Palomer, A.; Mauleón, D. Comparative Molecular Modeling Study of the Three-Dimensional Structures of Prostaglandin Endoperoxide H₂ Synthase 1 and 2 (COX-1 and COX-2). *J. Mol. Graphics* **1997**, *15*, 290–300.
- Kurumbail, R. G.; Stevens, A. M.; Gierse, J. K.; McDonald, J. J.; Stegeman, R. A.; Pak, J. Y.; Gildehaus, D.; Miyashiro, J. M.; Penning, T. D.; Seibert, K.; Isakson, P. C.; Stallings, W. C. Structural Basis for the Selective Inhibition of Cyclooxygenase-2 by Antiinflammatory Agents. *Nature* **1996**, *384*, 644–648.
- Marriott, D. P.; Dougall, I. G.; Meghani, P.; Liu, Y. J.; Flower, D. R. Lead Generation Using Pharmacophore Mapping and Three-Dimensional Database Searching: Application to Muscarinic M₃ Receptor Antagonists. *J. Med. Chem.* **1999**, *42*, 3210–3216.
- Willett, P. A Review of the 3-Dimensional Chemical-Structure Retrieval Systems. *J. Chemom.* **1992**, *6*, 289–305.
- Gillet, V. J.; Newell, W.; Mata, P.; Myatt, G.; Sike, S.; Zsoldos, Z.; Johnson, A. P. SPROUT: Recent Developments in the De Novo Design of Molecules. *J. Chem. Inf. Sci.* **1994**, *34*, 207–217.
- Ottoni, O.; Cruz, R.; Alves, R. Efficient and Simple Methods for the Introduction of the Sulfonyl, Acyl and Alkyl Protecting Groups on the Nitrogen of Indole and Its Derivatives. *Tetrahedron* **1998**, *54*, 13915–13928.
- Draheim, S. E.; Bach, N. J.; Dillard, R. D.; Berry, D. R.; Carlson, D. G.; Chirgadze, N. Y.; Clawson, D. K.; Hartley, L. W.; Johnson, L. M.; Jones, N. D.; McKinney, E. R.; Mihelich, E. D.; Olkowski, J. L.; Schevitz, R. W.; Smith, A. C.; Snyder, W.; Sommers, C. D.; Wery, J.-P. Indole Inhibitors of Human Nonpancreatic Secretory Phospholipase A₂. 3. Indole-3-glyoxamides. *J. Med. Chem.* **1996**, *39*, 5159–5175.
- Greene, J.; Kahn, S.; Savoj, H.; Sprague, P.; Teig, S. Chemical Function Queries for 3D Database Search. *J. Chem. Inf. Comput. Sci.* **1994**, *34*, 1297–1308.
- Reitz, D. B.; Isakson, P. C. Cyclooxygenase-2 Inhibitors. *Curr. Pharm. Des.* **1995**, *1*, 211–220.
- InsightII*, version 97, and *Discover*, version 2.98; Molecular Simulations, Inc.: San Diego, CA, 1997.
- Sprague, P. W. Automated Chemical Hypothesis Generation and Database Searching with Catalyst. In *Perspectives in Drug Discovery and Design*; Müller, K., Ed.; Escom: Leiden, The Netherlands, 1995; pp 1–20. Kaminski, J. J.; Rane, D. F.; Snow, M. E.; Weber, L.; Rothofsky, M. L.; Anderson, S. D.; Lin, S. L. Identification of Novel Farnesyl Protein Transferase Inhibitors Using Three-Dimensional Database Searching Methods. *J. Med. Chem.* **1997**, *40*, 4103–4112. Keller, P.; Bowman, M.; Dang, K. H.; Garner, J.; Leach, S. P.; Smith, R.; McCluskey, A. Pharmacophore Development for Corticotropin-Releasing Hormone: New Insights into Inhibitor Activity. *J. Med. Chem.* **1999**, *42*, 2351–2357.
- Brooks, B. R.; Bruccoleri, R. E.; Olafson, B. D.; States, D. J.; Swaminathan, S.; Karplus, M. CHARMm: A Program for Macromolecular Energy, Minimization and Dynamics Calculations. *J. Comput. Chem.* **1983**, *4*, 187–196.
- Smellie, A. S.; Teig, S. L.; Towbin, P. Poling: Promoting Conformational Variation. *J. Comput. Chem.* **1995**, *16*, 171–176.
- Smellie, A. S.; Kahn, S. D.; Teig, S. L. Analysis of Conformational Coverage. 1. Validation and Estimation of Coverage. *J. Chem. Inf. Comput. Sci.* **1995**, *35*, 285–292.

- (29) Smellie, A. S.; Kahn, S. D.; Teig, S. L. Analysis of Conformational Coverage. 2. Application of Conformational Models. *J. Chem. Inf. Comput. Sci.* **1995**, *35*, 295–301.
- (30) Riendeau, D.; Charleson, S.; Cromlish, W.; Mancini, J. A.; Wong, E.; Guay, J. Comparison of the Cyclooxygenase-1 Inhibitory Properties of Non-steroidal Anti-inflammatory Drugs (NSAIDs) and Selective COX-2 Inhibitors, Using Sensitive Microsomal and Platelet Assays. *Can. J. Physiol. Pharmacol.* **1997**, *75*, 1088–1095.
- (31) Carabaza, A.; Cabré, F.; Rotllan, E.; Gómez, M.; Gutiérrez, M.; García, M. L.; Mauleón, D. Stereoselective inhibition of inducible cyclooxygenase by chiral non-steroidal antiinflammatory drugs. *J. Clin. Pharmacol.* **1996**, *36*, 505–512.
- (32) *GraphPad PRISM*, version 2.0; GraphPad Software, Inc.: San Diego, CA, 1998.

JM010458R